

# Finding Symmetry in Intensity Images

R. Manmatha \*

Center for Intelligent Information Retrieval  
Computer Science Department,  
University of Massachusetts at Amherst, MA-01002  
manmatha@cs.umass.edu

Harpreet S. Sawhney  
Image Information Research Group,  
David Sarnoff Research Center,  
CN5300, Princeton, NJ-08543.  
sawhney@sarnoff.com

Keywords: Symmetry Detection, Gaussian Filters, Image Segmentation, Low Level Processing.

## Abstract

The salience of symmetry for patterns in the human visual system has been noted by a number of observers from Mach onwards. Psychophysical studies show that symmetry is important both for shape recognition and for figure-ground segregation. Here, a computational scheme for detecting local symmetry as an aid to detecting significant structures in images is presented. It is based on filtering with Gaussian derivatives.

---

\*Part of this research was done while the first author was visiting IBM and the second author was a Research Staff Member at IBM Almaden Research Center, San Jose, CA-95120. R. Manmatha's work is supported by in part by the National Science Foundation, Library of Congress and Department of Commerce under cooperative agreement number EEC-9209623, in part by the United States Patent and Trademarks Office and the Defense Advanced Research Projects Agency/ITO under ARPA order number D468, issued by ESC/AXS contract number F19628-95-C-0235 and in part by NSF Multimedia CDA-9502639. Any opinions, findings and conclusions or recommendations expressed in this material are the author(s) and do not necessarily reflect those of the sponsors.

The technique is shown to be applicable to intensity images as well as edge images and point sets. It is also shown how the method may be extended to detecting skew symmetry of rotational patterns. Finally, a brief discussion of related psychophysical work is presented.

## 1. Introduction

The salience of symmetry for patterns in the human visual system has been noted by a number of observers from Mach onwards. It has been speculated (theorized?) that symmetry places an important role in the perception of shape [19, 17]. Rock and others have argued that symmetry axes provide a local coordinate system which characterize a shape [19, 18]. Marr [17], for example, uses symmetry axes to assign an object-based coordinate system in the 2 1/2-D sketch. In computer vision, the role of (reflection) symmetry in defining shape has been explored by a number of researchers [3, 4, 5, 9]. Many of these methods [4, 3, 5] are based on point and line segment data that already correspond to a segmented object or pattern.

The presence of symmetry, however, is often a strong cue for figure-ground segregation in biological vision [21]. Symmetries can heavily influence the distinctiveness of an object/figure in relation to its background and. For example, the bodies of many animals are often characterized by a strong symmetry axis running from top to bottom. [18]. Symmetry may therefore be useful in object identification.

In this paper, we approach the problem of finding rotational and reflectional symmetries as an aid to detection of significant structure in an image. Given that one cannot rely on pre-segmented data for computing symmetries if segmentation is the goal, we propose the use of Gaussians and their derivatives at multiple scales as a way of detecting symmetries. This paper aims to demonstrate that symmetry axes can be detected using Gaussian derivatives. Their use in segmentation will be explored in a future paper. In general besides the useful symmetry axes, a symmetry detector will respond to homogeneous regions - which are trivially symmetric. Although broad homogeneous regions can be rejected with ease, narrow homogeneous regions are much harder to reject. This is because the edges of such

a homogeneous region will lie within any filter giving rise to a symmetric response. The narrow homogeneous region therefore gives rise to a ridge or valley. It is shown here that ridges and valleys are special kinds of symmetries and the symmetry detector will therefore respond to them.

Gaussian derivatives may be expressed in terms of Gaussian weighted moments. The conditions for rotational and reflectional symmetry using Gaussian weighted moments can be derived in the same manner as for “ordinary” moments [1]. An important advantage gained is that the scale associated with the Gaussian derivatives automatically limits the extent of the signal over which the moments are derived.

The importance of scale is demonstrated by the following example. Consider a 1-D signal which is symmetric over an interval  $[-a,a]$ . Outside of this interval the signal is not symmetric (see figure 1). “Ordinary” moments will not detect the symmetry because the entire signal is not symmetric. However, Gaussian weighted moments or Gaussian derivatives will detect the symmetry over a set of scales, if the scales are chosen to make the contributions of the asymmetric part negligible.

There is considerable evidence that primate visual systems use spatial filters at multiple scales in the early stages of processing. These are often modelled as Gabor or Gaussian derivative filters [20]. A number of different visual processes have been modelled using Gaussian derivative filters, for example, texture segmentation [15], blob detection [13], shape from texture [14]. The use of Gaussian derivative filters at multiple scales is, therefore, consistent with this paradigm and with data on the primate visual system. Further, psychophysical studies on symmetry show that [12, 18, 7]

1. symmetry detection is pre-attentive.



2. channel separation occurs before symmetry detection.
3. symmetry detection is local.
4. vertical and horizontal symmetry are detected most easily. Diagonal symmetry is detected with less ease.

The relationship of the scheme proposed here for detecting (reflection) symmetry with these psychophysical facts will be discussed later in the paper.

Since it is the Gaussians which are differentiated rather than the image itself, discontinuous images can be used for symmetry detection. Thus the method proposed to detect symmetry will detect them in edge images and point sets also. In principle the technique will also work on angle images - ie. images where the pixel values are replaced by the gradient angle. Thus a unified framework to detect all kinds of symmetries is provided.

Closely related to symmetry detection is the idea of detecting ridges and blobs. Ridges may be defined as reflection symmetries characterized by a bright bar surrounded by a dark background. Blobs are rotational symmetries characterized by a bright region wholly enclosed by a dark background.

Another interesting notion in symmetry is the idea of detecting skewed symmetry i.e. the symmetric pattern lies on a plane which is not parallel to the image plane. In the case of rotationally symmetric patterns, skewed symmetry imposes certain conditions on the Gaussian derivatives and these are derived.

This paper is organized as follows. First an intuitive notion of how symmetry can be characterized by the derivatives of a function is derived. this is formalized using the moments of an image is given. Since global moments over an image are rarely useful for detecting symmetry, the derivation is adapted to use Gaussian weighted moments. This is essentially

equivalent to using Gaussian derivatives. Images are rarely perfectly symmetric, rather they are approximately symmetric. The notion of approximate symmetry is discussed and is followed by a discussion of ridges and blobs. An algorithm for detecting symmetry in images is then provided and experiments on some real images are shown. The symmetry conditions discussed above are not only valid for image intensities, but also for edges and points and this is briefly discussed. The remaining sections of the paper discuss skew symmetry and how rotational skew symmetry can be detected.

## **1.1 Brief Review of Previous Work in Symmetry**

A fair amount of previous work in symmetry [3, 4, 5] assumes that the object has been previously segmented and an edge outline obtained. Local symmetry axes are then computed to obtain a shape description in terms of a line skeleton.

Although there has been a considerable amount of literature on symmetry in computer vision (see Zabrodsky [22] for a good review), very little has been concerned with using symmetry for segmentation in images. Reisfeld et al [8] developed a symmetry operator to find highly symmetric points in a face. They used this operator to detect faces. Zabrodsky [22] developed a general symmetry operator which she applied to detecting symmetry axes in faces. For an excellent review of previous work in computer vision on symmetry see

## **1.2 Contributions**

The contribution of this paper is to show that Gaussian derivatives at multiple scales can be used to detect reflection and rotation symmetry without any apriori segmentation. The use of Gaussian derivatives to detect skew symmetry for rotationally symmetric patterns is also derived. Experiments on real images are shown to illustrate these ideas. It is shown that ridges and valleys are special kinds of symmetries and they are also detected by the

symmetry detector.

## 2. Basic Ideas

An intuitive notion for characterizing symmetry can be obtained by looking at the derivatives of a function. Doing so provides an insight into the close connections between symmetry detection and finding ridges in images.

Consider a twice differentiable function  $F(x)$ . Let  $F(x)$  have a maximum at  $a$ . Then from elementary calculus

$$\nabla F(a) = 0 \tag{1}$$

and

$$F''(a) \leq 0 \tag{2}$$

Consider a 2D function  $f(x,y)$  which is mirror symmetric. Without loss of generality, assume that it is mirror symmetric about the  $y$ -axis. Consider the 1-D function  $f(x,b)$  for a fixed value of  $b$ . By mirror symmetry,  $f(x,b)$  must be even and hence can be written as

$$g(x) = f(x,b) = [f(x,b) + f(-x,b)]/2 \tag{3}$$

Now it is trivial to show that all the odd derivatives of  $g$  are odd functions and all the even derivatives of  $g$  are even functions. This implies that all the odd derivatives of  $g$  at  $x = 0$  must be zero and all the even derivatives of  $g$  attain their maximum at  $x = 0$ . It follows that all the odd derivatives have zero crossings at  $x = 0$ .

An implied assumption here is that the direction of the symmetry axis is known. The direction can be derived by finding the two principal second directional derivatives. The symmetry axis must lie along one of them. If the first derivative along the perpendicular direction is zero, then there is declared to be a valid symmetry axis. i.e. if  $x'$  or  $y'$  is a

symmetry axis  $[(x',y') = R(x,y)]$  then

$$R^T \nabla f = (0, k) \text{ or } (k, 0) \quad (4)$$

$$R^T f''(x, y) R = \Sigma \quad (5)$$

where  $\mathbf{R} = \mathbf{R}(\theta)$  is a 2-D rotation matrix and  $\Sigma$  is a 2 by 2 diagonal matrix. This definition is consistent with the symmetry conditions derived in the next section using moments. Thus symmetry is defined using the extremum values of the function  $f(x,y)$ .

One can deal with rotational symmetry in similar fashion. For example, let a function  $f(x,y)$  have rotational symmetry of order  $n$ . This implies that

$$f(\mathbf{x}) = f(R\mathbf{x}) \quad (6)$$

where  $R = R(\theta)$  is a 2D rotation matrix and  $\theta = 2\pi/n$ . Differentiating gives

$$\nabla f(\mathbf{x}) = R^T \nabla f(R\mathbf{x}) \quad (7)$$

and further differentiating gives

$$f''(\mathbf{x}) = R^T f''(R\mathbf{x}) R \quad (8)$$

Now the centers of rotational symmetries are fixed points and therefore

$$\nabla f(0) = R^T \nabla f(0) \quad (9)$$

$$f''(0) = R^T f''(0) R \quad (10)$$

which implies that  $\nabla f(0) = 0$  and  $f''(0) = k \mathbf{I}$ .

The notion of symmetry dealt with here is an infinitesimal one i.e. if  $f(x,y)$  is symmetric about the  $y$ -axis at  $(0,y)$ , then the neighbourhood over which this function is symmetric is  $(-\epsilon, \epsilon)$  i.e.  $f(\epsilon, y) = f(-\epsilon, y)$ . This is not very useful for a number of reasons. An image

has a large number of extremum points at a small scale - i.e. a large number of possible symmetries. Most symmetries in images, however, have finite extent and the interesting ones usually occur over much larger scales. It is, therefore, necessary to incorporate the notion of scale. It is also possible that a function, although even, may not be twice differentiable, so that the above symmetry conditions are not directly applicable. A third issue is the sensitivity of differentiation to noise at small scales. All these difficulties may be resolved by smoothing the image first with a Gaussian of an appropriate scale.

The notion of scale can be incorporated by smoothing with Gaussians at several scales and then differentiating to check for symmetry. Equivalently this involves directly convolving the image with Gaussian derivatives. The above derivation for symmetry conditions was based on an intuitive argument. A more formal derivation can be established using moments of the image. Moments provide global conditions on symmetry which are not very useful for many reasons. Most images are rarely globally symmetric, rather there are parts of them that are symmetric. Further, for most purposes one would like to derive an axis of symmetry which cannot be derived using the global conditions on moments. However, the derivation for moments can be adapted to use Gaussian weighted moments. Since Gaussian derivatives can always be expressed in terms of Gaussian weighted moments, symmetry conditions on Gaussian derivatives can also be derived from them.

### **3. Derivation Using Moments**

Symmetry can be used to derive conditions on the moments of a function. The easiest way to do this is to use complex moments. We will follow the derivation of Abu-Mostafa and Psaltis [1] here.

### 3.1 Derivation of the conditions for Rotational Symmetry

Define the complex moment  $C_{pq}$  of a function  $f(x,y)$  by

$$C_{pq} = \int (x + iy)^p (x - iy)^q f(x, y) dx dy \quad (11)$$

This may be expressed in polar coordinates as follows

$$\begin{aligned} C_{pq} &= \int r^p e^{ip\theta} r^q e^{-iq\theta} f(r, \theta) r dr d\theta \\ &= \int r^{p+q+1} e^{i\theta(p-q)} f(r, \theta) dr d\theta \end{aligned} \quad (12)$$

Let the pattern  $f(x,y)$  be rotated by an angle  $\phi$ . Then the new moment  $C'_{pq}$  can be expressed in terms of  $C_{pq}$  as

$$C'_{pq} = C_{pq} e^{i\phi(p-q)} \quad (13)$$

Both  $C_{pq}$  and  $C'_{pq}$  are complex numbers. Thus for  $(p - q) = 1$  there is a unique value of  $\phi$  for which  $C'_{pq}$  is positive real. This may be state in the form of a Lemma.

**Lemma 1** For  $(p - q) = 1$  there is a unique value of  $\phi, 0 \leq \phi \leq 2\Pi$  such that  $C'_{pq}$  is positive real.

**Lemma 2** Consider a  $k$ -fold rotationally symmetric pattern. By symmetry there must be  $k$  values of  $\phi$  for which  $C'_{pq}$  is positive real, where  $k$  is the order of symmetry.

**Lemma 3** Lemmas 1 and 2 can be consistent only if  $C'_{pq} = 0$  for any rotationally symmetric pattern ( $p - q = 1$ )

The general form of Lemma 3 when  $(p - q)$  is any integer can now be stated.

**Lemma 4** If a pattern is rotationally symmetric,  $C'_{pq} = 0$ , whenever the order of symmetry  $k$  does not divide  $(p - q)$ .

### 3.1.1 Examples

1. Let  $p = 1, q = 0$ . Then for any  $k \geq 1$  (i.e. any rotational symmetry)

$$C_{10} = \int \int (x + iy)f(x, y)dxdy = m_{10} + im_{01} = 0 \quad (14)$$

where  $m_{ab}$  denotes (ordinary) moments of order  $ab$ . Thus if the pattern is rotationally symmetric  $m_{10} = m_{01} = 0$ . This is another way of stating that the centroid of a rotationally symmetric pattern coincides with its center of symmetry.

2. Let  $p = 2, q = 0$ . Then for rotational symmetries of order 3 or greater,

$$C_{20} = \int \int (x + iy)^2 f(x, y)dxdy = m_{20} - m_{02} + i2m_{11} = 0 \quad (15)$$

Thus for rotational symmetry,  $m_{20} = m_{02}, m_{11} = 0$ . Define the second moment matrix by  $\begin{bmatrix} m_{20} & m_{11} \\ m_{11} & m_{02} \end{bmatrix}$ . Then it follows from the above that the second moment matrix must be the identity matrix times a constant.

## 3.2 Derivation of the conditions for Reflection Symmetry

Consider reflections about the  $x$  axis. Then  $C_{pq} = C_{pq}^*$ . This implies that  $C_{pq}$  must be real. Thus a reflection about the  $x$ -axis implies that  $C_{pq}$  must be real.

Reflections about any arbitrary axis can be obtained by first rotating the coordinate axis and then applying the above condition.

### 3.2.1 Examples

1.  $p = 1, q = 0$

$$C_{10} = \int \int (x + iy)f(x, y)dxdy = m_{10} + im_{01} \quad (16)$$

must be real. Thus  $m_{01} = 0$  for a reflection about the x-axis. Similarly for a reflection about the y-axis  $m_{10} = 0$ .

2.  $p = 2, q = 0$

$$C_{20} = \int \int (x + iy)^2 f(x, y)dxdy = m_{20} - m_{02} + i2m_{11} \quad (17)$$

must be real. Therefore  $m_{11} = 0$  for a reflection about the x-axis. The same condition holds for a reflection about the y-axis. Thus the second moment matrix for a reflection about the x or y axes must be diagonal.

The above derivations using moments were first noticed in the context of matching patterns under similarity transforms by Abu Mostafa and Psaltis [1]. They have not really been used to find symmetry for a number of reasons. First, for a reflection symmetry, one needs to derive a symmetry axis. However, all global moments do is show that whether the image is symmetric globally or not. They do not determine a symmetry axis. Images are rarely globally symmetric. Rather they may be symmetric over local regions. The notion of scale is, therefore, important both for reflection and rotation symmetries and this is not incorporated in the above derivations. This is, however, simple to do using Gaussian weighted moments. The derivation stays the same in this case. The derivation may then be modified to use Gaussian derivatives rather than Gaussian weighted moments.



## 4. Derivation Using Gaussian derivatives

One way to extend the above definitions is by first convolving the function  $f(x,y)$  with a Gaussian of an appropriate scale and then checking for the extrema. This is straightforward to do. Alternatively, this may be derived by defining Gaussian weighted moments.

A complex Gaussian weighted moment may be defined as

$$C'_{pq} = \int \int (x + iy)^p (x - iy)^q G(x, y, \sigma) f(x, y) dx dy \quad (18)$$

where  $G(x, y, \sigma)$  is a Gaussian. This definition implies that the symmetry conditions for Gaussian weighted moments remain the same as for regular moments.

The advantage gained is that a function which has rotational or reflection symmetry must satisfy this at several scales. The second advantage is that for reflection symmetries, symmetry axes will be obtained by computing the above moments at every point in the image.

A derivative of a Gaussian of any order may be expressed as a linear function of Gaussian weighted moments. Thus the symmetry conditions may now be modified and extended to Gaussian derivatives. Note that from this point onwards, only moments upto third order will be considered.

The first derivative of a Gaussian with respect to the x-axis are given by

$$\partial G(x, y, \sigma) / \partial x = -x / \sigma^2 G(x, y, \sigma) \quad (19)$$

and a similar expression holds for the y-derivative. Consider a function filtered with the first derivative of a Gaussian. This is equivalent to taking the first moments of the function at the same point. Therefore, the symmetry conditions at the point remain unchanged.

The second derivatives of a Gaussian are given by

$$\partial^2 G(x, y, \sigma) / \partial x^2 = x^2 / \sigma^4 G(x, y, \sigma) - G(x, y, \sigma) / \sigma^2 \quad (20)$$

$$\partial^2 G(x, y, \sigma) / \partial x \partial y = xy / \sigma^4 G(x, y, \sigma) \quad (21)$$

$$\partial^2 G(x, y, \sigma) / \partial y^2 = y^2 / \sigma^4 G(x, y, \sigma) - G(x, y, \sigma) / \sigma^2 \quad (22)$$

The second derivative matrix of a Gaussian may be defined as  $\begin{bmatrix} G_{xx} & G_{xy} \\ G_{xy} & G_{yy} \end{bmatrix}$ . The diagonal elements differ from the second moment matrix by the additional Gaussian terms. The second derivative matrix will be zero when the intensity is either constant or varies linearly within the support of the Gaussian. This follows from the linearity of convolution for then we have

$$F * G'' = F'' * G \quad (23)$$

Now  $F''$  is zero when  $F$  is either constant or linear, and hence it follows that  $F * G''$  is zero when  $F$  is constant or linear. Otherwise, the conditions for both reflection and rotation symmetry stay the same. This is useful, for it allows the elimination of patterns with uniform brightness. However, a bright bar

#### 4.1 Edges and Points.

Since it is the Gaussians that are differentiated rather than the image function itself, the above algorithm will detect symmetries in discontinuous images. Thus for example, it will detect symmetries in edge images and sets of points. However, for edge images it will produce symmetry axes at the edges. Although this is a symmetry axis for the edge image, it is not one for the original image. These extra axes are produced because the original intensity image which would have differentiated them is no longer available. An example of symmetry detection on an edge image is shown in

## 4.2 Scale Invariance of the Reflection Axes

Assume that the symmetry axis is invariant over a range of scales  $\sigma_0 \dots \sigma_m$ . Then all the first and second derivatives of Gaussians need to be rotated by the same matrix  $\mathbf{R}$  to obtain the axis of symmetry.

Proof: The first derivative conditions state that  $y'$  is the symmetry axis if  $G_{x',sigma} = 0$ . But  $(x', y') = \mathbf{R}^T(x, y)$  where  $\mathbf{R}$  is the rotation matrix. Note that  $\mathbf{R}$  does not depend on the scale but only the symmetry axis  $y'$  and the current coordinate system  $(x, y)$ . Since by assumption the symmetry axis is the same for  $\sigma_0 \dots \sigma_m$  it follows that  $\mathbf{R}$  must be the same for  $\sigma_0 \dots \sigma_m$ .

Corollary: Since the rotation matrix required to diagonalize the second derivative matrix is the same as required to diagonalize the first derivative matrix, it follows that  $\mathbf{R}$  must be the same for the second derivative matrix too.

## 5. Approximate Symmetry

Real images are rarely exactly symmetric. For example, the human face shows approximate bilateral symmetry. It is, therefore, important that the notion of symmetry formulated here capture this. Consider a 1-D function  $f(x)$  again. Assume that  $f(x)$  is approximately symmetric at  $(x = 0)$ . Convolve  $f(x)$  with a Gaussian  $G(x, \sigma)$  and let  $F(x) = f(x) * G(x, \sigma)$ . Let the scale  $\sigma$  be chosen such that  $F(x)$  is also approximately symmetric at  $(x = 0)$ . Let the even and odd parts of  $F(x)$  be  $E(x)$  and  $O(x)$ . Then

$$\nabla F(x) = \nabla E(x) + \nabla O(x). \quad (24)$$

At  $x = 0$ ,  $\nabla E(0) = 0$ , thus  $\nabla F(0) = \nabla O(0)$ . Similarly,  $F''(0) = E''(0)$ .

Therefore,  $O'(0)$  and  $E''(0)$ , in some sense, measure the deviation from symmetry. If they are large,  $F(x)$  is not symmetric at  $(x = 0)$  and if they are small, it is symmetric

about ( $x = 0$ ). Going to 2-D introduces another complicating factor - the orientation of the symmetry axis. If the orientation of the symmetry axis is assumed known, for example it is assumed vertical, then the above considerations still apply. However, if the orientation of the symmetry axis is unknown, this must also be recovered at the same time as symmetry is tested. For exactly symmetric patterns, this can be done by finding the rotation matrix which zeroes one of the components of  $\nabla F(x, y)$  and diagonalizes  $F''(x, y)$  at the same time. We will assume that this applies also to approximately symmetric patterns.

### 5.1 Ridges, Valleys and Blobs

Structure in images can also be defined in terms of ridges, valleys and blobs at multiple scales. The detected ridges and blobs can be used [2, 10, 14, 11] to segment the image. There is a close relationship between ridges, blobs and symmetric patterns. Ridges may be regarded as reflection symmetries defined by a single bright bar against a dark background (and valleys as dark bars against a light background). Circular blobs can be considered as special cases of rotationally symmetric patterns which are defined by a bright circular patch against a dark background (or vice-versa). Thus the symmetry conditions above also apply to ridges and valleys (a similar definition for ridges has been used by Burns et al [11]).

The optimal scale of a filter required to detect symmetry is hard to specify for general symmetries. However, for ridges and blobs, this can be specified by considering the filter outputs over a set of scales. The lowest filter which is useful for this purpose is the second derivative of Gaussian filter. This follows because a Gaussian convolution just produces the average value of the Gaussian weighted intensity while the first derivative filter produces zero at a point of symmetry. However, the second directional derivative perpendicular to the ridge must assume a maximum at some scale - and this scale can be assumed to be optimum. This scale therefore defines the extent of the symmetry (or ridge). The extent will depend on

the exact shape of the ridge. Here, it is derived for a ridge defined by a rectangular window. In a similar vein, Blostein and Ahuja [2] used the maximum of the Laplacian over scales to define circular blobs and Lindeberg and Garding [14] used the maximum of the trace of the hessian to specify the extent of elliptical blobs.

## 5.2 Derivation of the Extent of a Ridge

Consider a bright bar against a dark background. Let the ridge be infinite along one direction (say the y direction ) and in the perpendicular direction let it be defined by

$$F(x) = 1 \quad -k \leq x \leq k \quad (25)$$

$$= 0 \quad otherwise \quad (26)$$

Then consider the convolution of F with  $G_{xx}$ . At  $x = 0$ , the value of this convolution is

$$\int_{-k}^k (x^2/\sigma^2 - 1)/\sigma^2 G(x, \sigma) \quad (27)$$

This can be shown to attain a minimum with respect to scale (by differentiating the expression with respect to  $\sigma$ ) at  $k = \sqrt{(3)}\sigma$ . Thus the ridge has an extent of  $2k = 2\sqrt{(3)}\sigma$  when the convolution with respect to  $G_{xx}$  is a minimum with respect to scale.

Similar derivations can be carried out for other assumed shapes for the ridge.

## 6. Algorithm for finding Reflection Symmetry

The algorithm for detecting reflection symmetry will use the first two Gaussian derivatives. In general, the angle of the symmetry axis is unknown and therefore the second derivatives of the Gaussians are used to derive the angle. The zeroes of the first derivatives can then be used to locate the symmetry axes. The zeroes of the first derivatives are, however, not well localized for a couple of reasons. First, detection of a zero response requires some

kind of threshold and cannot therefore be well localized. Second, if a pattern is homogeneous in intensity, it will give zero responses over a large area. As discussed in section 2., a function which is exactly symmetric will have a zero crossing in its first derivative. Thus zero crossings can be used instead of zero responses. Zero crossings have the advantage of localization. A threshold on their slope is still needed to reject noise, but this threshold is not critical.

The algorithm for finding reflection symmetry may now be stated.

1. Convolve the image with first and second derivatives of Gaussians with standard deviation  $\sigma$ .
2. Diagonalize the second derivative matrix  $\mathbf{G}''$  i.e.

$$\mathbf{G}'' = \mathbf{R}^T(\theta)\mathbf{\Sigma}\mathbf{R}(\theta) \quad (28)$$

where  $\mathbf{R}(\theta)$  is a 2 by 2 rotation matrix and  $\mathbf{\Sigma}$  is a diagonal matrix (this follows from the symmetry of  $\mathbf{G}''$ ).

3. Now rotate the first derivative vector  $G_1'$  by the rotation matrix  $\mathbf{R}$  derived from the above diagonalization. i.e

$$\mathbf{G}' = \mathbf{R}^T\mathbf{G}_1' \quad (29)$$

4. Now look for zeroes in either of the first partial derivatives of  $\mathbf{G}'$ .

As discussed above, it is useful to modify the last step. Thus instead of looking for zeroes, we look for zero-crossings. Since noise could cause false zero crossings, these are then thresholded based on their slope - zero crossings which have small slope are rejected.

## 7. Experiments

On the top left in Figure 1 is a picture of a diskhead slider that has been twice reduced using a Gaussian pyramid. The lighting is almost but not completely uniform. The image was then filtered with Gaussian derivatives with  $\sigma = 5$ . On the top right is displayed the y derivative of the Gaussian while on the bottom right the y derivative is thresholded to show the zero crossings. The bottom left displays the detected symmetries using the above algorithm after thresholding the slope at 3. *The detected symmetry axes are all local.* No global curves have been fitted. As can be seen the symmetry axes are not all straight, but bend and curve around (the cross labels the corner of one of the bars). Note that the background between the metal strips also has symmetry axes. Figure and ground discrimination can be done by noting that the axes for the figure will have a positive second derivative along the direction of the symmetry axis.

Figure 2 shows the Lenna image frequently used in image processing. On the top left hand side is the original image reduced twice using a Gaussian pyramid. The image was again filtered with Gaussian derivatives with  $\sigma = 5$ . On the top right is the x derivative of the image and on the bottom right the zero crossings of the x derivative are shown. On the bottom left are the symmetry axes detected by the algorithm after thresholding the slope at 2. Many of these correspond to narrow homogeneous regions - in fact these are ridges and valleys and as discussed above ridges and valleys are special kinds of symmetries. (Since they are narrow, the edges of these regions lie within the filter. Thus they consist of a bright bar surrounded by a darker region which is the definition of a ridge (or dark against bright for valleys). The filters will, therefore, have a non-zero response to them. Broad homogeneous regions on the other hand will not respond to the filter. One of the symmetry axes corresponds to Lenna's face. This is indicated by the a line.

Figure 3 is almost identical except that the scale used is  $\sigma = 10$ . Note, that the number of axes is much reduced, but the axis defining the face is still present.

## 8. Determination of Skew Symmetry

Consider a symmetric pattern on a plane. If this plane is not parallel to the image plane, under weak perspective projection, the pattern's image will be skew symmetric. Skew symmetry causes the slant and tilt of the planes to be confounded with the symmetry conditions. For symmetric patterns, it can therefore be used to measure both the slant and tilt of the plane on which the pattern lies as well as for checking for symmetry.

Under weak perspective projection, the Gaussian derivatives on the plane and the image are related as follows [16]:

$$G'_1(., A^T A \sigma) = \mathbf{A}^T G'_0(., \sigma) \quad (30)$$

$$G''_1(., A^T A \sigma) = A^T G''_0(., \sigma) A \quad (31)$$

where symmetric projection matrix  $\mathbf{A} = s\mathbf{R}^T M \mathbf{R}$ .  $s$  is the scale,  $\mathbf{R}$  is a 2-D rotation matrix and  $M$  is the slant matrix given by

$$M = \begin{bmatrix} \cos\sigma & 1 \\ 0 & 1 \end{bmatrix} \quad (32)$$

Note that the Gaussian derivatives on the left hand side are elliptical while those on the right are circular. As a first approximation, it will be assumed that the Gaussians on the left-hand side can be approximated by circular Gaussian derivatives. The main problem (at least as far as detecting rotational skew symmetry) will be that the affine parameters will be estimated incorrectly. One can use an iterated procedure where the estimated affine parameters are used to refilter using elliptical Gaussians and the affine parameters reestimated.



## 8.1 Rotational Skew Symmetry

For rotational symmetry,  $G'_0 = 0$  and  $G''_0 = k\mathbf{I}$  for some constant  $k$ . Thus the above equations reduce to:

$$G'_1 = 0 \quad (33)$$

$$G''_1 = kA^T A \quad (34)$$

The eigenvalues of the second derivative matrix give the slant and tilt of the pattern [6]. Thus the slant and tilt of the plane are given by:

$$\cos\sigma = \sqrt{\frac{G_{xx} + G_{yy} - \sqrt{(G_{xx} - G_{yy})^2 + 4G_{xy}}}{G_{xx} + G_{yy} + \sqrt{(G_{xx} - G_{yy})^2 + 4G_{xy}}}} \quad (35)$$

$$\tan 2\tau = \frac{2G_{xy}}{G_{xx} - G_{yy}} \quad (36)$$

### 8.1.1 Algorithm for Detecting Rotational Skew Symmetry

1. Mark those places in the image where  $G'_1 = 0$ .
2. At those places compute the slant and tilt using the second derivative matrix.
3. Warp the image using the slant and tilt parameters and recompute.

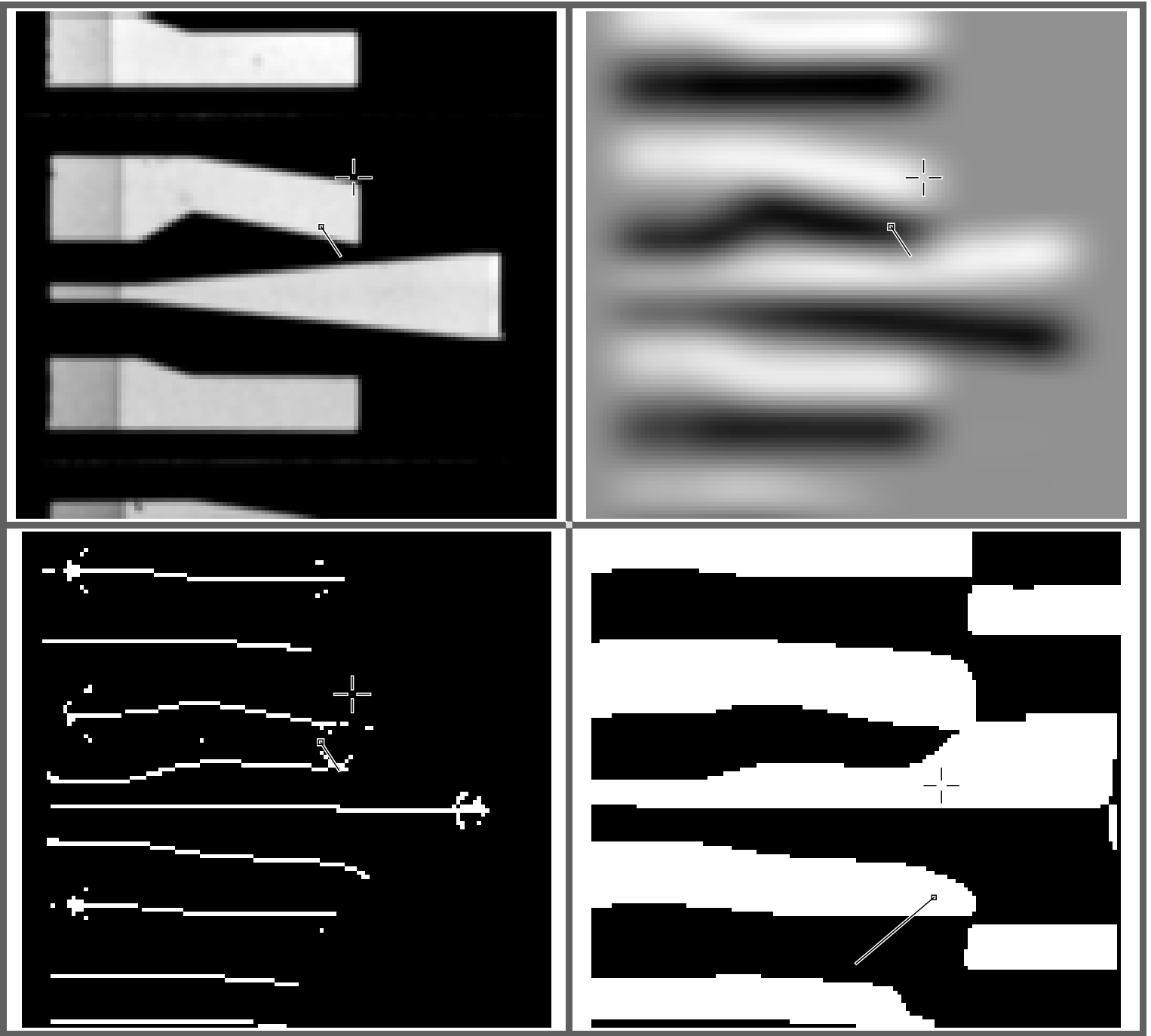
## 9. Consistency with psychophysical data

The computational theory for detecting symmetry that is proposed here is consistent with the psychophysical data on symmetry detection by humans. Consider first the experiments of Julesz and Chang [12]. They argued that separation into frequency channels occurs

before symmetry detection. They found that if two random dot patterns, one vertically symmetric and the other horizontally symmetric are added together, the resulting pattern is not perceived as symmetric. However, they found that if one of the patterns is low pass filtered and the other high pass filtered and the patterns are again added together, both symmetries are still perceived. If Gaussian derivatives of several different sigma's are used, the channel separation observed by Julesz and Chang will occur. The algorithm described here does filtering before symmetry detection which is consistent with the observations of Julesz and Chang [12]. Again, symmetry detection is considered local and pre-attentive which is consistent with the mechanisms suggested here.

There is considerable neurophysiological and psychophysical evidence that in the early stages of the primate visual system the input is filtered using spatial filters [20]. These have been modelled using gabor functions or Gaussian derivatives. The scheme proposed here is therefore, consistent with the available evidence in the use of such filters.

Corballis and Roldan [7] found that the time it took to verify that bilateral patterns are symmetric increased as the axis of symmetry was rotated from the vertical. The algorithm proposed, here, takes the same time for all rotational angles and is therefore not consistent with their evidence. However, a modified version of the algorithm would be consistent with such a scheme. A modified scheme could be generated as follows, the image is rotated by a set of discrete angles (say at steps of 15 deg). The first derivative of the Gaussian is then checked to see if it is close to zero - or has zero crossings. These are labelled as possible symmetries. Figure 4 shows an example of an image for which only the zero crossings in the vertical direction are displayed. Note that the faces are all detected as well as other ridges. Such a scheme would take time proportional to the rotational angle.



Top left: Slider image 2 reduced. Top Right:  $d/dy$  image. Bottom left: the detected bilateral symmetry Bottom right:  $d/dy$  showing the zero crossings.

Figure 1:



Top left: Lenna image 2 reduced. Top Right:  $d/dx$  image. Bottom left: the detected bilateral symmetry Bottom right:  $d/dx$  showing the zero crossings.

Figure 2:



Top left: Lenna image 2 reduced. Top Right:  $d/dx$  image. Bottom left: the detected bilateral symmetry Bottom right:  $d/dx$  showing the zero crossings.

Figure 3:



Left: Image, Right: x derivative thresholded

Figure 4:

## 10. References

- [1] Y.S. Abu-Mostafa and D. Psaltis. Recognitive aspects of moment invariants. *IEEE Transactions on Pattern Analysis and Machine Intelligence*, 6:698–706, 1984.
- [2] D. Blostein and N. Ahuja. A multiscale region detector. *Computer Vision Graphics and Image Processing*, 45:22–41, 1989.
- [3] H. Blum and R. Nagel. Shape description using weighted symmetric axis features. *Pattern Recognition*, 10:167–180, 1978.
- [4] F. L. Bookstein. The line-skeleton. *Computer Graphics and Image Processing*, 11:123–37, 1979.
- [5] M. Brady and H. Asada. Smoothed local symmetries and their implementations. *International Journal of Robotics Research*, 3(3):36–61, 1984.
- [6] L. Brown and H. Shvaytser. Surface orientation from projective foreshortening of isotropic texture autocorrelation. *IEEE Transactions on Pattern Analysis and Machine Intelligence*, 12(6):584–588, 1990.
- [7] M. C. Corballis and C. E. Roldan. Detection of symmetry as a function of angular orientation. *Journal of Experimental Psychology: Human Perception and Performance*, 1:221–230, 1973.
- [8] H. Wolfson D. Reisfeld and Y. Yeshurun. Robust facial feature detection using symmetry. In *Proc. International Conference on Pattern Recognition*, pages A:117–120, 1992.
- [9] J. M. Gauch and S. M. Pizer. The intensity axis of symmetry and its application to image segmentation. *IEEE Transactions on Pattern Analysis and Machine Intelligence*, 15(8):753–770, 1993.
- [10] J. M. Gauch and S. M. Pizer. Multiresolution analysis of ridges and valleys in grey-scale images. *IEEE Transactions on Pattern Analysis and Machine Intelligence*, 15(6):635–646, 1993.

- [11] H. K. Nishihara J. B. Burns and S. J. Rosenschein. Appropriate-scale local centers: a foundation for parts-based recognition. In *Proc. DARPA Image Understanding Workshop*, 1994.
- [12] B. Julesz and J. Chang. Symmetry perception and spatial-frequency channels. *Perception*, 8:711–718, 1979.
- [13] T. Lindeberg. Detecting salient blob-like image structures and their scales with a scale-space primal sketch. *International Journal of Computer Vision*, 11:283–318, 1993.
- [14] T. Lindeberg and J. Garding. Shape from texture from a multi-scale perspective. Technical Report Tech Rept. CVAP116, KTH, Stockholm, 1993.
- [15] J. Malik and P. Perona. Preattentive texture discrimination with early vision mechanisms. *Journal of the Optical Society of America A*, 7(5):923–932, 1990.
- [16] R. Manmatha. A framework for recovering affine transforms using points, lines or image brightnesses. In *Proc. Computer Vision and Pattern Recognition Conference*, pages 141–146, 1994.
- [17] D. Marr. *Vision*. W.H. Freeman: San Francisco, 1982.
- [18] H. Pashler. Coordinate frame for symmetry detection and object recognition. *Journal of Experimental Psychology: Human Perception and Performance*, 16:150–163, 1990.
- [19] I. Rock. *Orientation and Form*. Academic Press: New York, 1973.
- [20] R. L. De Valois and K. K. De Valois. *Spatial Vision*. Oxford University Press: New York, 1988.
- [21] M. Wertheimer. Principles of perceptual organization. In D.C. Beardslee and M. Wertheimer, editors, *Readings in Perception*. Van Nostrand: Princeton, 1958.
- [22] H. Zabrodsky. *Computational Aspects of Pattern Characterization - Continuous Symmetry*. PhD thesis, Hebrew University, Jerusalem, 1993.